

## Ultrafast Electron Pulses from a Tungsten Tip Triggered by Low-Power Femtosecond Laser Pulses

Peter Hommelhoff, Catherine Kealhofer, and Mark A. Kasevich

Physics Department, Stanford University, Stanford, California 94305, USA

(Received 30 June 2006; published 14 December 2006)

We present an experimental and numerical study of electron emission from a sharp tungsten tip triggered by sub-8-fs low-power laser pulses. This process is nonlinear in the laser electric field, and the nonlinearity can be tuned via the dc voltage applied to the tip. Numerical simulations of this system show that electron emission takes place within less than one optical period of the exciting laser pulse, so that an 8 fs 800 nm laser pulse is capable of producing a single electron pulse of less than 1 fs duration. Furthermore, we find that the carrier-envelope phase dependence of the emission process is smaller than 0.1% for an 8 fs pulse but is steeply increasing with decreasing laser pulse duration.

DOI: [10.1103/PhysRevLett.97.247402](https://doi.org/10.1103/PhysRevLett.97.247402)

PACS numbers: 78.47.+p, 42.79.Hp, 79.70.+q

Fast, laser driven electron sources are crucial as photoelectron injectors for accelerators and free electron lasers [1]. They have also enabled time-resolved imaging of fundamental processes in such diverse fields as solid state physics [2,3], chemistry [4], and biology [5]. Because of the nature of the emission processes utilized so far, the electron pulses at best resemble the laser pulse *envelope* and are usually more than 100 fs long. Ultrafast sub-laser-cycle ( $\sim 1$  fs) electron sources have recently been obtained in laser-ionization of gas phase atoms [6]. However, a spatially localized source with sub-laser-cycle resolution has been unknown so far. Here we demonstrate a spatially and temporally localized source of ultrafast electron pulses. The electron pulses are generated by the carrier electric field of a three cycle laser pulse and are emitted from a sharp field emission tip to confine the source area down to nanometric dimensions. This electron source should find application in novel optical accelerators [7], in new interferometers, and in all kinds of ultrafast electron microscopy [8].

Our system consists of a field emission tip onto which we focus sub-8 fs laser pulses with sufficiently large field strengths that optical field emission dominates the emission process. In previous work, we have studied laser-induced field emission using longer ( $\sim 70$  fs) laser pulses [9]. For such long pulses, the electrons are expected to be emitted over a time that is comparable to the length of the exciting laser pulse. However, for few cycle laser pulses, optical field emission can lead to electron emission in a time set by the laser *period* so that the emitted electron pulse is significantly shorter than the laser pulse itself. Optical field emission from solids is the direct analog to optical tunnel ionization in atoms [10], with the distinct advantage that the emitted electrons originate from an area determined by the tip dimension (on the order of nanometers) and not by the laser spot size (typically microns), and that the electron beam from a field emission tip is well collimated down to about  $10^\circ$ .

Considered from a different point of view, the electron emission processes described above can be used to probe the exciting laser *electric field*, in stark contrast to more conventional sensors that probe the laser intensity and average over at least one optical period in the laser field. This distinction becomes important for laser pulses shorter than three optical periods, and critical for pulses that are close to or in extreme cases even shorter than one optical period [11]. The value of the electric field is usually parametrized by the carrier-envelope phase angle, which describes the phase advance of the electric carrier field with respect to the pulse envelope [10]. In this work, we study optical field emission from a tungsten tip both from the perspective of generating ultrashort electron pulses and from the perspective of developing a simple carrier-envelope phase detector.

In our setup a tungsten tip in (111) orientation with a radius of curvature of around 80 nm is mounted in an ultrahigh vacuum chamber (Fig. 1). A Kerr-lens mode-locked Ti:sapphire laser generates laser pulses with a repetition rate of 150 MHz and an average output power of around 500 mW. We measure the pulse duration with a standard doubling crystal autocorrelator to be below but close to 8 fs (for more details see [12]). The laser beam traverses a dispersion balanced interferometer [13], which

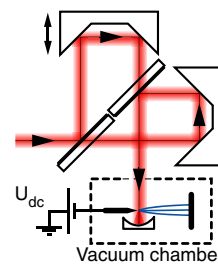


FIG. 1 (color online). Sketch of the experimental setup. The laser beam traverses a dispersion balanced interferometer, whose output is focused onto the field emission tip.

allows the measurement of interferometric autocorrelation traces using the field emission tip as a nonlinear element (Fig. 1). The output beam from the interferometer is focused on the tip with a spherical gold mirror to a spot radius of  $\sim 4 \mu\text{m}$  ( $1/e^2$ ). The tip is oriented perpendicular to the laser beam direction, and the polarization vector of the laser light is parallel to the tip shank. Emitted electrons are accelerated towards an imaging microchannel plate detector and the amplified current is measured. In addition to the laser electric field, it is possible to add a dc field to the tip by applying a voltage  $U_{\text{dc}}$ . For sharp tips, the electric field  $F$  and the applied voltage  $U$  are related by the equation  $F = U/(kr)$ , with the tip radius  $r$  and the geometric factor  $k \approx 5$  [14]. With an average laser power of  $\sim 100$  mW, electric field strengths of around 0.75 GV/m can be generated in the focal spot. Because the dimensions of the tip are smaller than the laser wavelength, ac field enhancement takes place. We expect an enhancement factor of around 4 so that the electric field at the tip can reach 3 GV/m [9,15].

Figure 2(a) shows three interferometric autocorrelation traces (IATs) recorded in the electron current for three different dc electric fields but identical laser parameters. We observe that the emission current for two pulses that are separated by  $\sim 100$  fs is additive. This rules out the possibility that the nonlinearity in the emission process is due to thermionic emission. Thermionic emission scales exponentially with the deposited laser energy [14] and has typical time scales of 100 fs to 1 ps [16]. Adjusting the dc field causes the shape of the IAT's to change because the nonlinearity of the emission process increases in a continuous manner as the dc field is reduced. To quantify this, we divide the peak emission current by the baseline current and plot this ratio versus the dc field [Fig. 2(b)]. For  $F_{\text{dc}} =$

0.53 GV/m the peak-to-baseline ratio reaches 25, which should be compared with peak-to-baseline ratios of 8 and 32 for conventional second and third order processes.

The dashed curve shows a semiquantitative model for the data based on optical field emission. In the optical field emission regime, the tunnel current at a given time can be viewed as that arising from dc tunneling with the electric field given by the sum of the applied dc field and the instantaneous value of the laser field. The dc tunneling is described by the Fowler-Nordheim equation [14], which relates the tunnel current  $I$  to the applied electric field  $F$ :

$$I = AF^2 \exp\left(-\frac{B}{F}\right), \quad (1)$$

with  $A$  and  $B$  about constant. Because of the exponential nonlinearity in this equation, the photocurrent obtained at the maximum of the laser electric field ( $F_{\text{laser}}$ ) makes the largest contribution to the total emission probability. This is given by

$$I_{\text{base}} = 2A(F_{\text{laser}} + F_{\text{dc}})^2 \exp\left(-\frac{B}{F_{\text{laser}} + F_{\text{dc}}}\right) \quad (2)$$

for two nonoverlapping laser pulses and

$$I_{\text{peak}} = A(2F_{\text{laser}} + F_{\text{dc}})^2 \exp\left(-\frac{B}{2F_{\text{laser}} + F_{\text{dc}}}\right) \quad (3)$$

for two perfectly overlapping identical pulses. We fit the ratio of Eq. (2) and (3) to the data of Fig. 2 with  $F_{\text{laser}}$  as free parameter. The model fits the data reasonably well (dashed red curve in Fig. 2) and we obtain as best fit value  $F_{\text{laser}} = 1.8 \pm 0.2$  GV/m, which is consistent with the parameters of our system given the uncertainty in the size of the laser focus and field enhancement factor.

The Fowler-Nordheim theory used above describes field emission in steady state for a dc field. For time-dependent processes, in particular, for processes involving laser pulses with durations comparable to electronic time scales in metals, this model might prove to be insufficient. In order to include key dynamical effects, we have integrated the one-dimensional time-dependent Schrödinger equation. The potential is modeled as shown in Fig. 3, where the size of the box is chosen such that the ground state wave function matches the electronic Fermi energy in tungsten. This model reflects the fact that field emission from (111) planes should be dominated by emission from surface states [17]. The effect of the laser field is to modulate the barrier so that the potential reads  $V(z, t) = V_0 = -13.5$  eV inside the metal ( $z \leq 0$ ) and  $V(z, t) = -q^2/(16\pi\epsilon_0 z) - qz[F_{\text{dc}} + F_0 \exp(-2 \ln t^2/\tau^2) \cos(\omega t + \phi)]$  outside. Here, the first term is the image potential,  $F_0$  is the peak of the laser electric field envelope,  $F_{\text{dc}}$  is the applied dc field,  $z$  the spatial coordinate, and  $\phi$  the carrier-envelope phase angle. We find the initial ground state wave function (in absence of the tunnel barrier:  $F_0 = F_{\text{dc}} = 0$ ) with the imaginary time method. The simulation

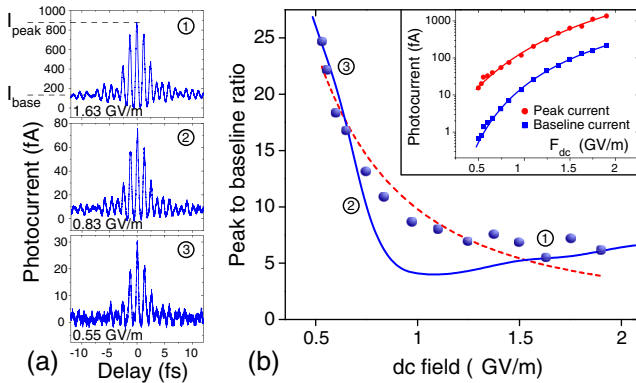


FIG. 2 (color online). Autocorrelation traces with tunable nonlinearity. (a) Autocorrelation traces for three different dc voltages but identical laser parameters. (b) Peak-to-baseline ratio vs dc tip voltage (blue points: data). The solid blue line is the simulation result with no adjustable parameter; the dashed red line is a fit of the simple optical field emission model to the data. The numbers in circles correspond to the traces given in (a). Inset: peak current and baseline current vs dc tip voltage.

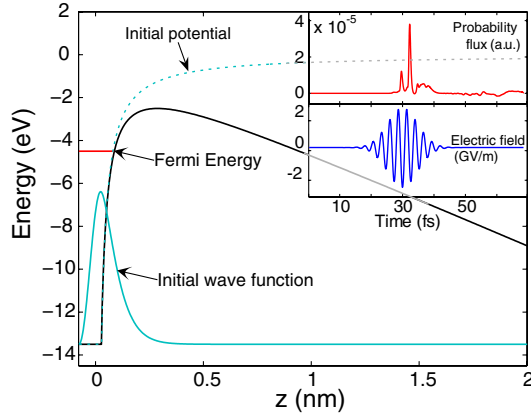


FIG. 3 (color online). Model and electron pulse. Model potential used in the calculations, shown here with an applied electric field of  $F = 4.4$  GV/m (solid black line).  $E = 0$  is the vacuum energy. Initial potential and initial wave function are shown in light blue. The inset shows the electric field generated by a three cycle laser pulse ( $F_{\text{laser}} \approx 2.7$  GV/m,  $F_{\text{dc}} = 0.2$  GV/m, CE phase  $\phi = \pi$ , bottom), and the resulting probability flux (top). A single electron pulse with a width of 660 as (FWHM) is emitted. The measurement position was at  $z = 2$  nm for this plot.

records the probability flux at  $z \approx 6$  nm outside of the metal for each time step. With this method, we calculate the probability current integrated over a single laser pulse as a function of pulse duration, pulse energy, dc tip voltage, and carrier-envelope (CE) phase.

From tunnel current versus fluence behavior we extract the nonlinearity and calculate the expected peak-to-baseline ratio. The result is the solid blue line in Fig. 2, a theory curve with no adjustable parameters. Given that our model does not include any properties of the emitter material other than the work function, the agreement with the data is very good. From this and also from the agreement of the simple model described earlier we infer that it is optical field emission that dominates the emission process. The slight deviations in both models might be due to competing processes, owing to the fact that the Keldysh parameter  $\gamma$  in our experiment is of order 1, which means that the emission process is not expected to be simply described in the limits of either the quasistatic or the perturbative regime ( $\gamma \ll 1$  or  $\gamma \gg 1$ , respectively) [10].

In optical field emission, individual laser cycles are expected to be resolved because electrons are preferentially emitted at the electric field maxima of the laser pulse. For a long pulse there are several spikes in the electron emission, but this structure should quickly be lost upon propagation of the electrons. Therefore, right after emission the upper limit of the electron pulse duration is given by the laser pulse duration. Because optical field emission is nonlinear (see autocorrelation traces in Fig. 2), the electron emission duration is expected to be shorter than the laser pulse duration, and can, for sub-3-cycle pulses,

shrink to emission of electrons during one optical period only. In the simulation, we obtain isolated sub-laser-cycle electron pulses for a wide range of parameters (inset in Fig. 3). For our experimental conditions, this would correspond to electron emission times of around 660 as. Future work will seek to directly measure the electron emission duration.

In principle, optical field emission is extremely sensitive to the electric field of the laser pulse. Because of the exponential in Eq. (1), optical tunnel emission was the prominent process envisioned to enable a direct measurement of carrier-envelope effects [18]. Although several sensors for the CE phase of ultrashort laser pulses exist [19–21], none of these allows direct CE phase locking of the laser. Miniaturized, a detector like the one used in this work could be used as such a system, with the observable being a modulation in the emission current depending on  $\phi$ . Figure 4 shows the modulation depth [minimum current (as function of  $\phi$ ) subtracted from maximum current divided by the sum] as a function of pulse energy and dc field for a two-cycle pulse. The largest modulation depth (21%) lies close to the origin and stays on that order of magnitude on a ridge that runs under a small angle to the fluence axis.

Figure 5 displays the modulation depths for laser pulses with different pulse durations. Contour plots for each pulse duration show similar behaviors to the one shown in Fig. 4. We find that for a three cycle pulse the carrier-envelope phase modulates the emission current by no more than 0.1%. In contrast, a time-independent Fowler-Nordheim calculation yields an almost 1 order of magnitude larger modulation depth. We have studied the problem experimentally by locking the carrier-envelope frequency of our laser using an  $f$ - $2f$  interferometer [22] and looking for a signal at the carrier-envelope frequency in the emitted electron current. Our detection system was sensitive to a modulation depth of down to  $\sim 0.1\%$ . We did not observe a carrier-envelope signal at this level with three cycle laser pulses. The discrepancy between the time-dependent and

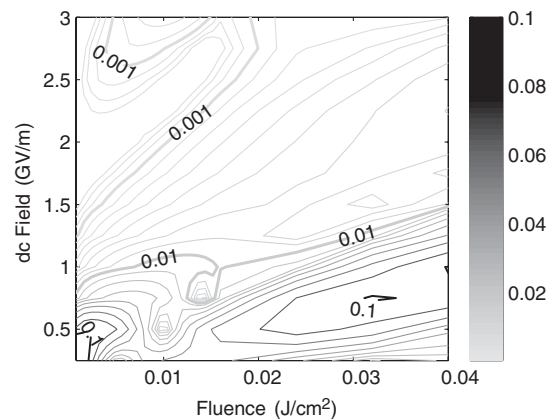


FIG. 4. Contour plot (log scale) of the modulation depth as a function of dc field and fluence for a 2 cycle laser pulse ( $\tau = 5.3$  fs). Line spacing is 8 contours per decade.

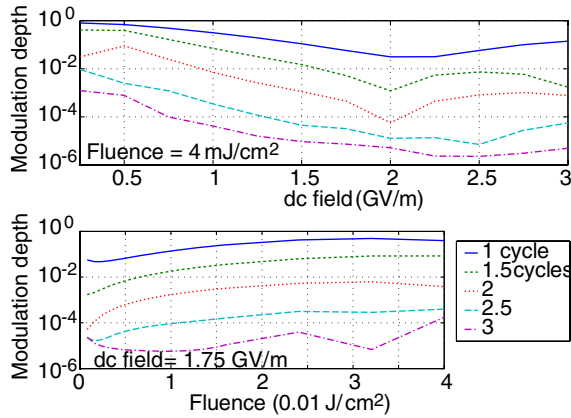


FIG. 5 (color online). Modulation depth as a function of dc field and fluence for different pulse durations.

the time-independent calculation presumably stems from the fact that the barrier modulation time scale is comparable to the barrier tunneling time. We conclude that a field emitter based sensor is less suitable than initially expected [18]. However, based on the simulation results, we find that for pulses shorter than  $\sim 2$  optical periods a field emitter based system will represent a good carrier-envelope phase detector.

CE phase stabilized lasers have been shown to possess a timing jitter of down to 40 as [23,24]. With such a system and a simulated electron emission duration of 660 as, the timing jitter of the emission can be expected to lie well in the attosecond to femtosecond domain. Evidently, a finite initial energy spread and Coulomb repulsion will lead to a loss of timing accuracy. Fast acceleration of the electrons to energies  $\geq 100$  keV, a limitation to one electron per pulse [5], and laser-induced dispersion control will mitigate these effects. An electron source with such a high time resolution would be extremely desirable for future laser accelerators, in which the commonly used microwave acceleration field will be replaced by an optical frequency electric field [7], and photonic crystal waveguides will take the place of microwave cavities [25,26]. Additionally, time-resolved imaging of biological, chemical, and solid state processes with faster and brighter electron sources will push forward knowledge in each respective field [2–4].

We would like to thank Steve Harris's group and MenloSystems for lending us equipment and Phil Bucksbaum for discussions. This work was supported by grants from the ARO MURI program and by the Humboldt Foundation (P.H.).

[1] V. Ayvazyan, N. Baboi, I. Bohnet, and R. Brinkmann *et al.*, Phys. Rev. Lett. **88**, 104802 (2002).

- [2] M. Merano, S. Sonderegger, A. Crottini, and S. Collin *et al.*, Nature (London) **438**, 479 (2005).
- [3] B.J. Siwick, J.R. Dwyer, R.E. Jordan, and R.J.D. Miller, Science **302**, 1382 (2003).
- [4] H. Ihee, V.A. Lobastov, U.M. Gomez, B.M. Goodson, R. Srinivasan, C.-Y. Ruan, and A.H. Zewail, Science **291**, 458 (2001).
- [5] V.A. Lobastov, R. Srinivasan, and A.H. Zewail, Proc. Natl. Acad. Sci. U.S.A. **102**, 7069 (2005).
- [6] H. Niikura, F. Légère, R. Hasbani, A.D. Bandrauk, M.Y. Ivanov, D.M. Villeneuve, and P.B. Corkum, Nature (London) **417**, 917 (2002).
- [7] T. Plettner, R.L. Byer, E. Colby, B. Cowan, C.M.S. Sears, J.E. Spencer, and R.H. Siemann, Phys. Rev. Lett. **95**, 134801 (2005).
- [8] W.E. King, G.H. Campbell, A. Frank, B. Reed, J.F. Schmerge, B.J. Siwick, B.C. Stuart, and P.M. Weber, J. Appl. Phys. **97**, 111101 (2005).
- [9] P. Hommelhoff, Y. Sortais, A. Aghajani-Talesh, and M.A. Kasevich, Phys. Rev. Lett. **96**, 077401 (2006).
- [10] T. Brabec and F. Krausz, Rev. Mod. Phys. **72**, 545 (2000).
- [11] M.Y. Shverdin, D.R. Walker, D.D. Yavuz, G.Y. Yin, and S.E. Harris, Phys. Rev. Lett. **94**, 033904 (2005).
- [12] P. Hommelhoff, C. Kealhofer, and M.A. Kasevich, in Proceedings of the 2006 IEEE International Frequency Control Symposium (to be published).
- [13] C. Spielmann, L. Xu, and F. Krausz, Appl. Opt. **36**, 2523 (1997).
- [14] V.T. Binh, N. Garcia, and S.T. Purcell, Adv. Imaging Electron Phys. **95**, 63 (1996).
- [15] Y.C. Martin, H.F. Hamann, and H.K. Wickramasinghe, J. Appl. Phys. **89**, 5774 (2001).
- [16] D.M. Riffe, X.Y. Wang, M.C. Downer, D.L. Fisher, T. Tajima, and J.L. Erskine, J. Opt. Soc. Am. B **10**, 1424 (1993).
- [17] T. Ohwaki, H. Ishida, and A. Liebsch, Phys. Rev. B **68**, 155422 (2003).
- [18] L. Xu, C. Spielmann, A. Poppe, T. Brabec, F. Krausz, and T.W. Hänsch, Opt. Lett. **21**, 2008 (1996).
- [19] G.G. Paulus, F. Lindner, H. Walther, A. Baltuška, E. Goulielmakis, M. Lezius, and F. Krausz, Phys. Rev. Lett. **91**, 253004 (2003).
- [20] A. Apolonski, P. Dombi, G.G. Paulus, and M. Kakehata *et al.*, Phys. Rev. Lett. **92**, 073902 (2004).
- [21] T.M. Fortier, P.A. Roos, D.J. Jones, S.T. Cundiff, R.D.R. Bhat, and J.E. Sipe, Phys. Rev. Lett. **92**, 147403 (2004).
- [22] R. Holzwarth, T. Udem, T.W. Hänsch, J.C. Knight, W.J. Wadsworth, and P.S.J. Russell, Phys. Rev. Lett. **85**, 2264 (2000).
- [23] T. Fuji, J. Rauschenberger, A. Apolonski, and V.S. Yakovlev *et al.*, Opt. Lett. **30**, 332 (2005).
- [24] O.D. Mücke, R. Ell, A. Winter, J.W. Kim, J.R. Birge, L. Matos, and F.X. Kärtner, Opt. Express **13**, 5163 (2005).
- [25] X.E. Lin, Phys. Rev. ST Accel. Beams **4**, 051301 (2001).
- [26] B.M. Cowan, Phys. Rev. ST Accel. Beams **6**, 101301 (2003).